

# Mapping New Realities: Ground Truth Image Creation with Pix2Pix Image-to-Image Translation

1<sup>st</sup> Zhenglin Li

Department of Computer Science and Engineering  
Texas A&M University  
College Station, TX, USA  
zhenglin\_li@tamu.edu

2<sup>nd</sup> Bo Guan

College of Science  
Virginia Tech  
Blacksburg, VA, USA  
jasonguan0107@gmail.com

4<sup>th</sup> Yiming Zhou

Department of Engineer Sciences  
Saarland University of Applied Sciences  
Saarbruecken, Germany  
yiming.zhou@htwsaar.de

3<sup>rd</sup> Yuanzhou Wei

Department of Electrical and Computer Engineering  
Florida International University  
Miami, FL, USA  
ywei011@fiu.edu

5<sup>th</sup> Jingyu Zhang

Division of the Physical Sciences  
The University of Chicago  
Chicago, IL, USA  
simonajue@gmail.com

6<sup>th</sup> Jinxin Xu

Department of Cox Business School  
Southern Methodist University  
Dallas, TX, USA  
jensenjxx@gmail.com

**Abstract**—Generative Adversarial Networks (GANs) have significantly advanced image processing, with Pix2Pix being a notable framework for image-to-image translation. This paper explores a novel application of Pix2Pix to transform abstract map images into realistic ground truth images, addressing the scarcity of such images crucial for domains like urban planning and autonomous vehicle training. We detail the Pix2Pix model’s utilization for generating high-fidelity datasets, supported by a dataset of paired map and aerial images, and enhanced by a tailored training regimen. The results demonstrate the model’s capability to accurately render complex urban features, establishing its efficacy and potential for broad real-world applications.

**Index Terms**—Machine Learning, Computer Vision, Generative Adversarial Networks

## I. INTRODUCTION

The advent of Generative Adversarial Networks (GANs) has revolutionized the field of image processing, enabling new heights of image synthesis and transformation [1]–[4]. Among these advancements, the Pix2Pix framework has emerged as a pivotal methodology for image-to-image translation tasks, particularly in applications that require a high degree of accuracy and detail, such as the construction of ground truth images from cartographic data. This paper introduces a novel application of Pix2Pix, leveraging its conditional adversarial network structure to transform abstract map images into detailed, realistic ground truth images, which has a lot of real-world applications [5].

This research is rooted in the premise that accurate ground truth images are indispensable across numerous domains, from urban planning and simulation to autonomous vehicle training and geographical information systems. However, the scarcity of such images often poses a significant barrier. By employing the Pix2Pix model, we propose a scalable solution to this scarcity, with the potential to automate and enhance the generation of high-fidelity ground truth datasets.

## II. RELATED STUDY

The challenge of synthesizing photorealistic images from schematic representations is multifaceted, involving not only the faithful reproduction of spatial information but also the nuanced translation of textures, patterns, and contextual details. Pix2Pix addresses this challenge by conditioning the generation process on input images, herein maps, and guiding the generative model with a discriminator that assesses the verisimilitude of the output against the actual ground truth. The discriminator’s role is crucial, as it pushes the generator towards creating outputs that are increasingly indistinguishable from real-world imagery.

Convolutional Neural Networks (CNNs) have been instrumental in advancing image processing tasks, providing a foundational architecture for many generative models [6], [7]. Recently, image to image translation presents a promising result. Among those popular image to image translation models, Adversarial Training play a significant role.

## III. METHODOLOGY

### A. Data Preparation

In the initial stage of our research, we compiled a dataset comprising pairs of images: one representing a map and the other its corresponding real-world aerial view, the ground truth. These images were processed using TensorFlow’s I/O and image decoding functions to load and pair JPEG images accurately. The images were split and cast into floating-point tensors to facilitate further operations [8], [9].

### B. Image Preprocessing

To enhance the robustness of our model, we applied random jittering and normalization to the input data. The random jittering process involves resizing the images to 286x286 pixels and cropping them to the final size of 256x256 pixels [10], [11]. Furthermore, we randomly mirror the images on the horizontal axis. The normalization step adjusts the pixel values

to a  $[-1, 1]$  range, which is a standard practice aimed at promoting training convergence [12]–[14].

### C. Model Architecture

Our model architecture is based on the Pix2Pix framework, which consists of a generator and a discriminator [15]. The generator aims to transform an input image into an output image, while the discriminator tries to distinguish between the real target image and the generated image.

### D. Generator

The generator is a U-Net-like architecture with an encoder-decoder structure [16]. Fig. 1 shows such architecture.

The encoder consists of a series of convolutional layers with downsampling, and the decoder consists of a series of transposed convolutional layers with upsampling. Skip connections are used between corresponding layers in the encoder and decoder to help preserve spatial information [17].

The encoder consists of the following layers:

- Convolutional layer with 64 filters, kernel size of 4, stride of 2, and no batch normalization.
- Convolutional layers with 128, 256, 512, 512, 512, 512, and 512 filters, each with a kernel size of 4, stride of 2, and batch normalization.

The decoder consists of the following layers:

- Transposed convolutional layers with 512 filters, kernel size of 4, stride of 2, batch normalization, and dropout.
- Transposed convolutional layers with 512, 512, 512, 256, 128, and 64 filters, each with a kernel size of 4, stride of 2, and batch normalization.
- Transposed convolutional layer with 3 output channels (for RGB images), kernel size of 4, stride of 2, and a tanh activation function.

The output of the generator,  $G(x)$ , for an input image  $x$  is given by:

$$G(x) = \tanh(W_n * \dots \sigma(W_2 * \sigma(W_1 * x + b_1) + b_2) \dots + b_n) \quad (1)$$

where  $W_i$  and  $b_i$  are the weights and biases of the  $i$ -th layer and  $\sigma$  is the activation function.

### E. Discriminator

The discriminator is a PatchGAN classifier, tailored for tasks involving paired input and target images to do the image translation. It consists of input layers, concatenation layer, three downsampling layers, convolutional layers, zero padding layers, batch normalization layer, activation layers using LeakyReLU, and final convolutional layer. Fig. 2 shows such architecture.

- Input Layers: Two input layers for the input image and the target image, each with a shape of  $[256, 256, 3]$ .
- Concatenation Layer: Combines the input and target images along the channel dimension, resulting in a shape of  $[256, 256, 6]$ .

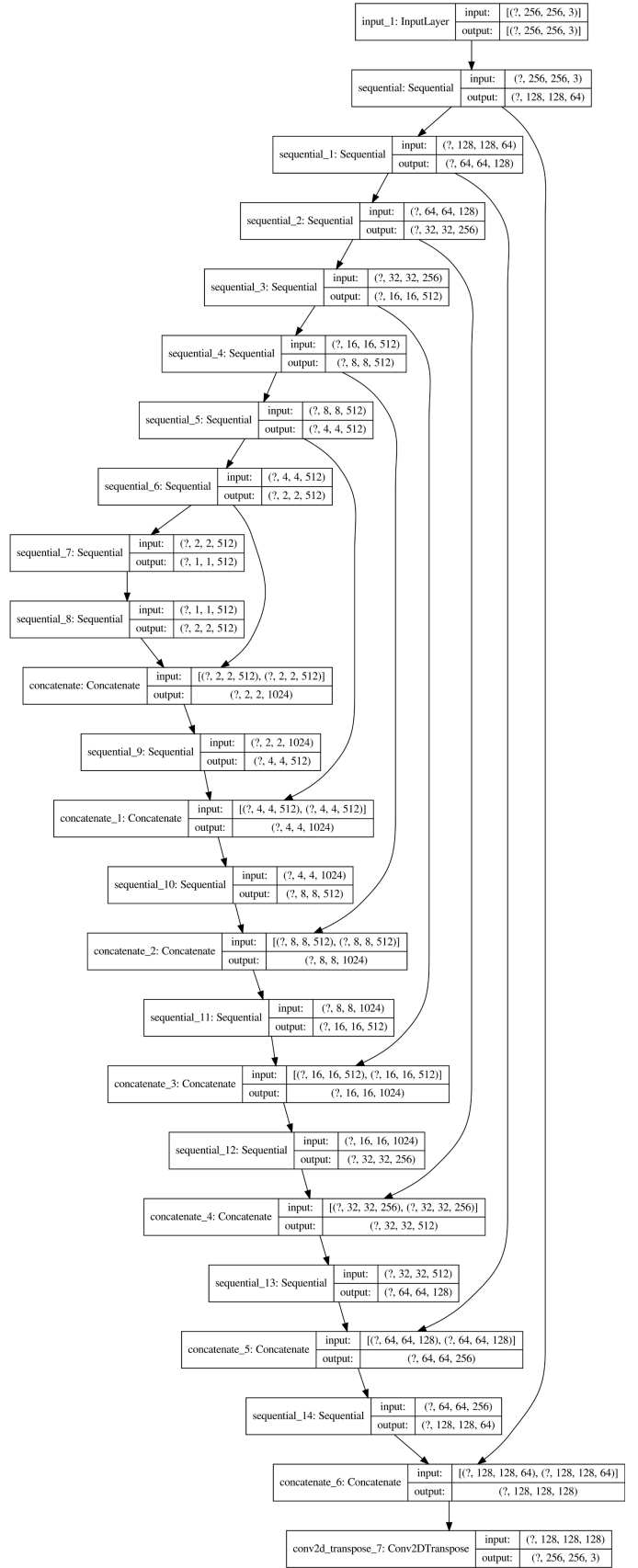


Fig. 1. The Architecture of Generator. It is a U-Net-like architecture with an encoder-decoder structure.

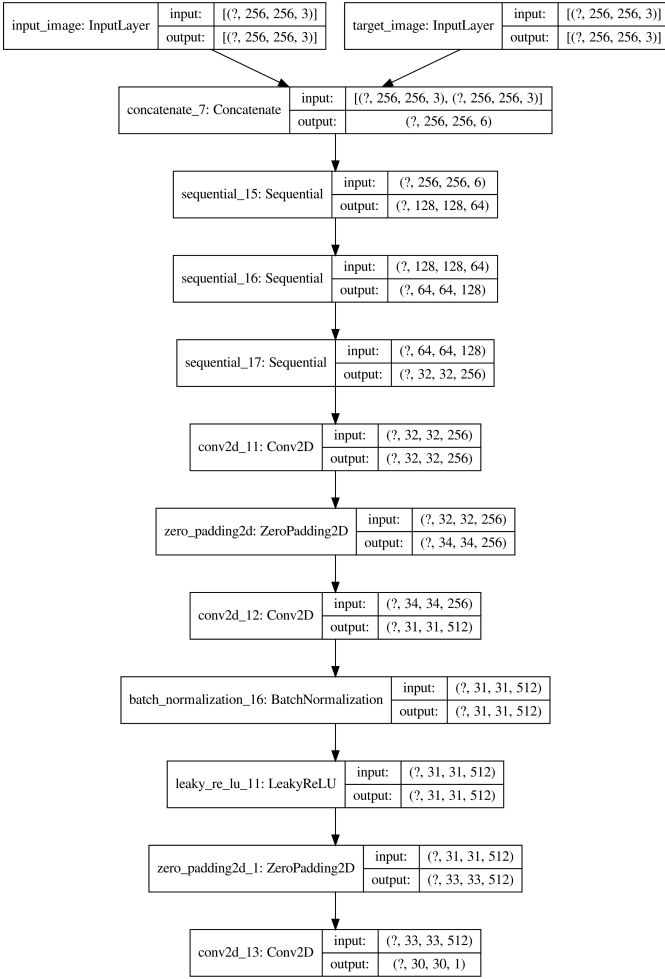


Fig. 2. The Architecture of Discriminator

- **Downsampling Layers:** First downsample reduces dimensions to [128, 128, 64], with 64 filters and a kernel size of 4. Second downsample further reduces dimensions to [64, 64, 128], with 128 filters. Third downsample reduces dimensions to [32, 32, 256], with 256 filters.
- **Convolutional Layers:** A convolutional layer with 256 filters and kernel size of 3, activation function relu and another convolutional layer with 512 filters, kernel size of 4, and strides of 1, without bias units, initiated with a specific kernel initializer.
- **Zero Padding Layers:** One ZeroPadding2D applied after the first convolutional layer (256 filters) to adjust the spatial dimensions before further processing. And another ZeroPadding2D applied after the LeakyReLU activation, prior to the final convolutional operation.
- **Batch Normalization Layer:** BatchNormalization applied after the second convolutional layer (512 filters) to normalize the activations of the previous layer.
- **Activation Layers:** LeakyReLU provides a non-linear activation function that allows a small gradient when the unit is not active.

- **Final Convolutional Layer:** A final convolutional operation with 1 filter, kernel size of 4, and strides of 1 to produce a single-channel output.

The discriminator takes as input the concatenation of the input image and the target/generated image and outputs a single scalar value representing the probability that the input image-target pair is real. Both the generator and discriminator use Leaky ReLU activation functions and are initialized with random normal weights with a mean of 0 and a standard deviation of 0.02.

The output of the discriminator,  $D(x, y)$ , for an input image  $x$  and target image  $y$  is given by:

$$D(x, y) = \sigma \left( W_m * \dots * \sigma \left( W_2 * \sigma \left( W_1 * \begin{bmatrix} x \\ y \end{bmatrix} + b_1 \right) + b_2 \right) \dots + b_m \right) \quad (2)$$

where  $[x, y]$  denotes the concatenation of  $x$  and  $y$ , and  $W_i$  and  $b_i$  are the weights and biases of the  $i$ -th layer.

## IV. EXPERIMENT AND RESULT

During the experiment, we evaluated the performance of the Pix2Pix model in translating abstract map representations into corresponding ground truth images. The model was trained on a dataset comprising various urban and rural landscapes to ensure robustness and generality in the translation capability [18].

### A. Training Procedure

The training is conducted iteratively, alternating updates between the generator and discriminator using TensorFlow's gradient computation and application functionalities. This process is repeated across several epochs, with periodic generation of images to visually monitor translation quality [19].

### B. Optimization Strategy

We employ the Adam optimizer for both generator and discriminator, with a learning rate of  $2e-4$  and a momentum parameter  $\beta_1$  set to 0.5. This choice is made to facilitate stable training and convergence.

### C. Result Visualization

Furthermore, we present a series of figure comparisons to illustrate the model's translation capability. Fig. 3 showcase the three sets of input maps, ground truth, and Pix2Pix-generated images. These visual results highlight the model's proficiency in generating coherent and contextually accurate urban imagery.

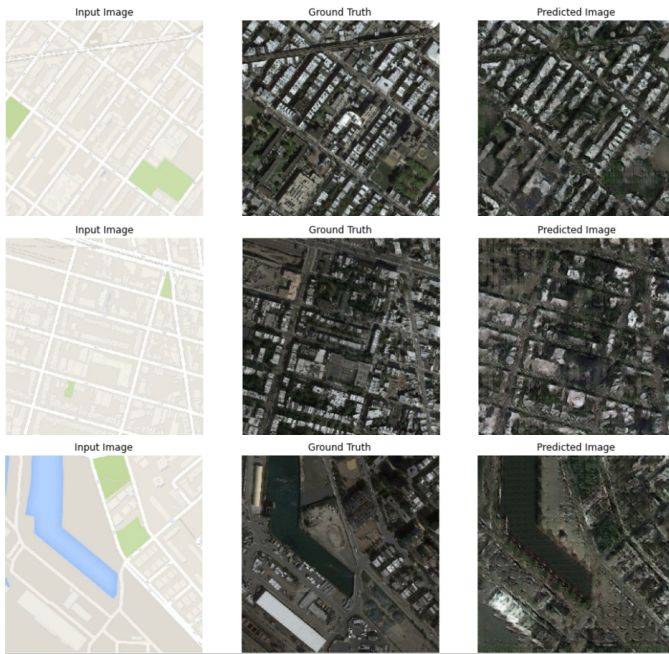


Fig. 3. Result Visualization

## V. LIMITATIONS AND FUTURE WORK

The results from our experiments with the Pix2Pix model confirm its potential as a powerful tool for map-to-image translation tasks. The ability to generate detailed and accurate ground truth images from abstract representations holds significant promise for various applications, including urban planning, simulation environments, and geospatial analysis.

Despite the promising results, the model exhibited limitations in certain scenarios. Specifically, regions with homogeneous textures or repetitive patterns occasionally resulted in artifacts in the generated images.

Future work may explore the integration of more sophisticated loss functions and training strategies to enhance the model's performance and reduce the incidence of translation artifacts. Further investigations could delve into the utilization of advanced loss functions that are specifically tailored to address the unique challenges of the domain, thereby potentially yielding higher quality translations [20]. Additionally, exploring a variety of training strategies, such as adaptive learning rate schedules or the use of transfer learning [21], could significantly improve the model's ability to generalize across different contexts. Beyond traditional methods, the incorporation of transformer-based models [22]–[24], multi-modal approaches [25], [26], vision-language integrations [27]–[30], and reinforcement learning techniques could offer promising avenues for research. These methods may not only refine the accuracy but also broaden the scope of the model's applicability to more complex scenarios, enhancing its robustness and effectiveness.

## VI. CONCLUSION

In this study, we have demonstrated the effective application of the Pix2Pix model to transform abstract map images into highly detailed and realistic ground truth images, suitable for use in urban planning and autonomous vehicle training. The Pix2Pix framework, employing a conditional adversarial network, has shown remarkable capability in accurately rendering complex urban landscapes and features from simple cartographic inputs.

Our experiments highlight the model's robustness and its potential to significantly alleviate the scarcity of high-fidelity ground truth datasets, a critical barrier in numerous domains. By leveraging a dataset of paired map and aerial images and optimizing our training procedures, we achieved impressive results that validate the practical utility of the Pix2Pix model.

Overall, our findings support the Pix2Pix model's potential as a transformative tool for image-to-image translation tasks, opening avenues for its application in diverse fields that rely on accurate and detailed visual data representations.

## REFERENCES

- [1] A. Creswell, T. White, V. Dumoulin, K. Arulkumaran, B. Sengupta, and A. A. Bharath, "Generative adversarial networks: An overview," *IEEE signal processing magazine*, vol. 35, no. 1, pp. 53–65, 2018.
- [2] J. Liao, V. Sanchez, and T. Guha, "Self-supervised frontalization and rotation gan with random swap for pose-invariant face recognition," in *2022 IEEE International Conference on Image Processing (ICIP)*, pp. 911–915, IEEE, 2022.
- [3] J. Liao, T. Guha, and V. Sanchez, "Self-supervised random mask attention gan in tackling pose-invariant face recognition," *Available at SSRN 4583223*.
- [4] X. Yin, S. Li, and G. K. Rohde, "Learning energy-based models with adversarial training," in *European Conference on Computer Vision*, pp. 209–226, Springer, 2022.
- [5] C. Zhan, M. Ghaderibaneh, P. Sahu, and H. Gupta, "Deepmtl: Deep learning based multiple transmitter localization," in *2021 IEEE 22nd International Symposium on a World of Wireless, Mobile and Multimedia Networks (WoWMoM)*, pp. 41–50, IEEE, 2021.
- [6] H. Wang, F. Yuan, L. Gao, R. Huang, and W. Wang, "Wear debris classification and quantity and size calculation using convolutional neural network," in *Cyberspace Data and Intelligence, and Cyber-Living, Syndrome, and Health: International 2019 Cyberspace Congress, CyberDI and CyberLife, Beijing, China, December 16–18, 2019, Proceedings, Part I 3*, pp. 470–486, Springer, 2019.
- [7] W. Ding, S. Li, G. Zhang, X. Lei, and H. Qian, "Vehicle pose and shape estimation through multiple monocular vision," in *2018 IEEE International Conference on Robotics and Biomimetics (ROBIO)*, pp. 709–715, IEEE, 2018.
- [8] Y. Wang, J. Wu, N. Hovakimyan, and R. Sun, "Balanced training for sparse gans," *Advances in Neural Information Processing Systems*, vol. 36, 2024.
- [9] C. Li, X. Lin, Y. Mao, W. Lin, Q. Qi, X. Ding, Y. Huang, D. Liang, and Y. Yu, "Domain generalization on medical imaging classification using episodic training with task augmentation," *Computers in biology and medicine*, vol. 141, p. 105144, 2022.
- [10] Z. Zhu and W. Zhou, "Taming heavy-tailed features by shrinkage," in *International Conference on Artificial Intelligence and Statistics*, pp. 3268–3276, PMLR, 2021.
- [11] Y. Lai, Z. Luo, and Z. Yu, "Detect any deepfakes: Segment anything meets face forgery detection and localization," in *Chinese Conference on Biometric Recognition*, pp. 180–190, Springer, 2023.
- [12] S. Sun, W. Ren, T. Wang, and X. Cao, "Rethinking image restoration for object detection," *Advances in Neural Information Processing Systems*, vol. 35, pp. 4461–4474, 2022.

- [13] Q. Jia, Y. Liu, D. Wu, S. Xu, H. Liu, J. Fu, R. Vollgraf, and B. Wang, "Kg-flip: Knowledge-guided fashion-domain language-image pre-training for e-commerce," in *Proceedings of the 61st Annual Meeting of the Association for Computational Linguistics (Volume 5: Industry Track)*, pp. 81–88, 2023.
- [14] L. Li, "Cpseg: Finer-grained image semantic segmentation via chain-of-thought language prompting," in *Proceedings of the IEEE/CVF Winter Conference on Applications of Computer Vision*, pp. 513–522, 2024.
- [15] P. Isola, J.-Y. Zhu, T. Zhou, and A. A. Efros, "Image-to-image translation with conditional adversarial networks," in *Proceedings of the IEEE conference on computer vision and pattern recognition*, pp. 1125–1134, 2017.
- [16] J. Zhuang, M. Gao, and M. A. Hasan, "Lighter u-net for segmenting white matter hyperintensities in mr images," in *Proceedings of the 16th EAI International Conference on Mobile and Ubiquitous Systems: Computing, Networking and Services*, pp. 535–539, 2019.
- [17] Q. Zhou, S. Guo, J. Pan, J. Liang, J. Guo, Z. Xu, and J. Zhou, "Pass: Patch automatic skip scheme for efficient on-device video perception," *IEEE Transactions on Pattern Analysis and Machine Intelligence*, 2024.
- [18] L. Wang, R. Benmokhtar, and X. Perrotton, "Interactive deep annotation as daros: Object detection supervision for efficient instance segmentation," in *International Conference on Image Analysis and Processing*, pp. 528–540, Springer, 2022.
- [19] H. Sun, X. Liu, X. Feng, C. Liu, N. Zhu, S. J. Gjerswold-Selleck, H.-J. Wei, P. S. Upadhyayula, A. Mela, C.-C. Wu, *et al.*, "Substituting gadolinium in brain mri using deepcontrast," in *2020 IEEE 17th International Symposium on Biomedical Imaging (ISBI)*, pp. 908–912, IEEE, 2020.
- [20] D. Zhang, F. Zhou, Y. Wei, X. Yang, and Y. Gu, "Unleashing the power of self-supervised image denoising: A comprehensive review," *arXiv preprint arXiv:2308.00247*, 2023.
- [21] X. Wang and Y. Jin, "Transfer reinforcement learning: Feature transferability in ship collision avoidance," in *International Design Engineering Technical Conferences and Computers and Information in Engineering Conference*, vol. 87318, p. V03BT03A071, American Society of Mechanical Engineers, 2023.
- [22] F. Lin, X. Yuan, Y. Zhang, P. Sigdel, L. Chen, L. Peng, and N.-F. Tzeng, "Comprehensive transformer-based model architecture for real-world storm prediction," in *Joint European Conference on Machine Learning and Knowledge Discovery in Databases*, pp. 54–71, Springer, 2023.
- [23] M. Li, P. Ling, S. Wen, X. Chen, and F. Wen, "Bubble-wave-mitigation algorithm and transformer-based neural network demodulator for water-air optical camera communications," *IEEE Photonics Journal*, 2023.
- [24] Y. Liu, H. Liu, L. Li, Z. Wu, and J. Chen, "A data-centric solution to nonhomogeneous dehazing via vision transformer," in *Proceedings of the IEEE/CVF Conference on Computer Vision and Pattern Recognition*, pp. 1406–1415, 2023.
- [25] W. Lyu, X. Dong, R. Wong, S. Zheng, K. Abell-Hart, F. Wang, and C. Chen, "A multimodal transformer: Fusing clinical notes with structured ehr data for interpretable in-hospital mortality prediction," in *AMIA Annual Symposium Proceedings*, vol. 2022, p. 719, American Medical Informatics Association, 2022.
- [26] F. Lin, S. Crawford, K. Guillot, Y. Zhang, Y. Chen, X. Yuan, L. Chen, S. Williams, R. Minvielle, X. Xiao, *et al.*, "Mmst-vit: Climate change-aware crop yield prediction via multi-modal spatial-temporal vision transformer," in *Proceedings of the IEEE/CVF International Conference on Computer Vision*, pp. 5774–5784, 2023.
- [27] Y. Zhou, X. Li, Q. Wang, and J. Shen, "Visual in-context learning for large vision-language models," *arXiv preprint arXiv:2402.11574*, 2024.
- [28] H. Chen, W. Huang, Y. Ni, S. Yun, F. Wen, H. Latapie, and M. Imani, "Taskclip: Extend large vision-language model for task oriented object detection," *arXiv preprint arXiv:2403.08108*, 2024.
- [29] Y. Xin, S. Luo, H. Zhou, J. Du, X. Liu, Y. Fan, Q. Li, and Y. Du, "Parameter-efficient fine-tuning for pre-trained vision models: A survey," *arXiv preprint arXiv:2402.02242*, 2024.
- [30] Y. Chen, C. Liu, W. Huang, S. Cheng, R. Arcucci, and Z. Xiong, "Generative text-guided 3d vision-language pretraining for unified medical image segmentation," *arXiv preprint arXiv:2306.04811*, 2023.